Current Biology, Vol. 13, 1660–1668, September 30, 2003, ©2003 Elsevier Science Ltd. All rights reserved. DOI 10.1016/j.cub.2003.08.032

A Determinant for Directionality of Organelle Transport in *Drosophila* Embryos

Steven P. Gross,[1,2] Yi Guo,[3,5] Joel E. Martinez,[2] and Michael A. Welte[3,4,*]
[1]Department of Developmental and Cell Biology
2222 Natural Sciences I
University of California Irvine
Irvine, California, 92697
[2]Department of Biomedical Engineering
204 Rockwell Engineering Center
University of California Irvine
Irvine, California 92697
[3]Rosenstiel Biomedical Research Center
[4]Department of Biology
[5]Department of Biochemistry
Brandeis University
450 South Street
Waltham, Massachusetts 02454

Summary

Background: Motor-driven transport along microtubules is a primary cellular mechanism for moving and positioning organelles. Many cargoes move bidirectionally by using both minus and plus end-directed motors. How such cargoes undergo controlled net transport is unresolved.
Results: Using a combination of genetics, molecular biology, and biophysics, we have identified Halo, a novel regulator of lipid droplet transport in early *Drosophila* embryos. In embryos lacking Halo, net transport of lipid droplets, but not that of other cargoes, is specifically altered; net transport is minus-end directed at developmental stages when it is normally plus-end directed. This reversal is due to an altered balance of motion at the level of individual organelles; without Halo, travel distances and stall forces are reduced for plus-end and increased for minus-end motion. During development, *halo* mRNA is highly upregulated just as net plus-end transport is initiated (phase II), and its levels drop precipitously shortly before transport becomes minus-end directed (phase III). Exogenously provided Halo prevents the switch to net minus-end transport in phase III in wild-type embryos and induces net plus-end transport during phase II in *halo* mutant embryos. This mechanism of regulation is likely to be of general importance because the *Drosophila* genome encodes a family of related proteins with similar sequences, each transiently expressed in distinct domains.
Conclusions: We conclude that Halo acts as a directionality determinant for embryonic droplet transport and is the first member of a new class of transport regulators.

Introduction

Motor-driven transport along microtubules is a primary mechanism that cells employ to move and position organelles [1]. Many cargoes move bidirectionally by using both minus and plus end-directed motors. Despite frequent back-and-forth motion, these cargoes display carefully controlled net displacement over time [2–4].

How is such net transport regulated? In a cell-culture model system, the transport of pigment granules in melanophores, net transport is controlled by a global cAMP-mediated signaling cascade that operates through PKA [5]. Even in this best-understood model system, the functionally relevant downstream targets of the signaling cascade have not been identified.

During development, proper control of timing and directionality of cargo transport is especially crucial because different cargoes are delivered to distinct embryonic locations simultaneously. It is unclear to what extent such transport regulation relies on signaling cascades as characterized in cultured cells or whether developmental regulation of protein expression also plays an important role.

We previously developed a model system to analyze such motor regulation: lipid-droplet transport during *Drosophila* embryogenesis [3, 6]. Droplets move bidirectionally along microtubules: the minus-end motor is cytoplasmic dynein; the plus-end motor remains to be identified. Motors are coordinated to prevent a tug-of-war between opposite-polarity motors on the same cargo, and this coordination requires both the dynein cofactor dynactin [7] and the regulator Klar [3].

Net transport of lipid droplets depends on the relative travel distances of plus- and minus-end runs (periods of uninterrupted motion) and changes twice over a 2 hr period. Initially, travel distances are balanced, with no net transport (phase I, syncytial blastoderm). Upregulation of plus-end travel distances before cellularization (phase II) leads to net plus-end inward transport. During gastrulation (phase III), plus-end transport is downregulated, whereas minus-end motion remains constant, resulting in net minus-end transport and droplets moving back toward the periphery. Because these changes in net transport are stereotypic and consistently occur at the same time during embryogenesis [3], they are likely to be due to developmentally controlled signaling events. The molecules that mediate these signals and their precise effect on the transport machinery are unknown.

Here we demonstrate that the transition from phase I to phase II involves two distinct events: a transcription-independent signal and the expression of a small, basic protein, Halo. Halo is cargo-specific, alters motion at the level of individual organelles, and determines the direction of net transport. This type of regulation is likely to be of general importance because there exists a whole family of Halo-related proteins.

Results

Transcription of Embryonic Genes Is Required for Cytoplasmic Clearing in Phase II

In *Drosophila*, many of the mRNAs and proteins that drive early development are maternally provided. When

*Correspondence: welte@brandeis.edu

we injected embryos with the transcription inhibitor α-amanitin before the onset of zygotic transcription (before phase I), they developed apparently normally until early phase II but then failed to cellularize, as previously reported [8]. Lipid droplets still moved bidirectionally. Thus, the basic machinery that transports droplets (e.g., tracks, motors, adaptors) is supplied maternally.

However, the peripheral cytoplasm of α-amanitin-treated embryos failed to clear, resulting in a hazy, brownish halo around the central, dark yolk (Figures 1A–1E). In contrast, the periphery of uninjected or mock-injected embryos became progressively transparent. Such altered transparency is a signature for mislocalized lipid droplets [3, 6]. We confirmed that droplets had failed to move inward by staining with the droplet-specific dye Oil Red O (not shown). Thus, net plus-end droplet transport in phase II requires new transcription of one or more genes.

Clearing Requires Zygotic Expression of the *halo* Locus

Embryos that lack DNA from the 22AB region of chromosome II also fail to undergo cytoplasmic clearing [9], suggesting that a single locus, provisionally named *halo* [9], is necessary zygotically to initiate clearing. Using 20 deletions with breakpoints in this region, we mapped *halo* to chromosomal bands 22A2–3. We combined one deletion with a chromosomal duplication to construct a synthetic deletion, Δ(*halo*). Embryos homozygous for Δ(*halo*) failed to clear in phase II (Figures 2A and 2B). Unexpectedly, these embryos yielded viable and fertile adults, enabling us to derive a homozygous Δ(*halo*) stock. Thus, neither a failure to clear nor the complete lack of *halo* leads to lethality.

The Δ(*halo*) deletion allowed us to ask if clearing required both maternal and zygotic *halo* function. When Δ(*halo*) females were crossed to wild-type males, embryos cleared in phase II. Thus, zygotic expression from a single copy of *halo* is sufficient to initiate net plus-end transport. Conversely, when the mothers carried zero, one, or two copies of wild-type *halo* but the embryos lacked *halo* (see also [9]), embryos failed to clear. Thus, only the zygotic expression of *halo* is crucial for net plus-end transport in phase II. This analysis suggests that Halo acts in *trans* to regulate the maternally provided transport machinery.

Halo Determines the Net Directionality of Droplet Transport

Lack of clearing in the absence of Halo might be due to general problems with the microtubule tracks and motors, it might affect a range of transport processes, or it might specifically alter droplet transport. Microtubule directionality and extent were apparently unaffected because the distribution of a plus-end marker was indistinguishable between the two genotypes (Figure 2C). Apart from lipid droplets, other markers examined showed a normal distribution (Figure 2). Δ(*halo*) embryos proceeded through cellularization, gastrulation, and germband extension apparently normally and completed embryogenesis. The Δ(*halo*) defect is specific for lipid droplets and thus makes it possible to analyze how one regulatory factor controls a single, defined transport process.

In the mutant embryos, lipid droplets accumulated apically during phase II, just below the nuclei (Figures 2F and 2G), as previously noted from electron microscopy in embryos with large deletions encompassing

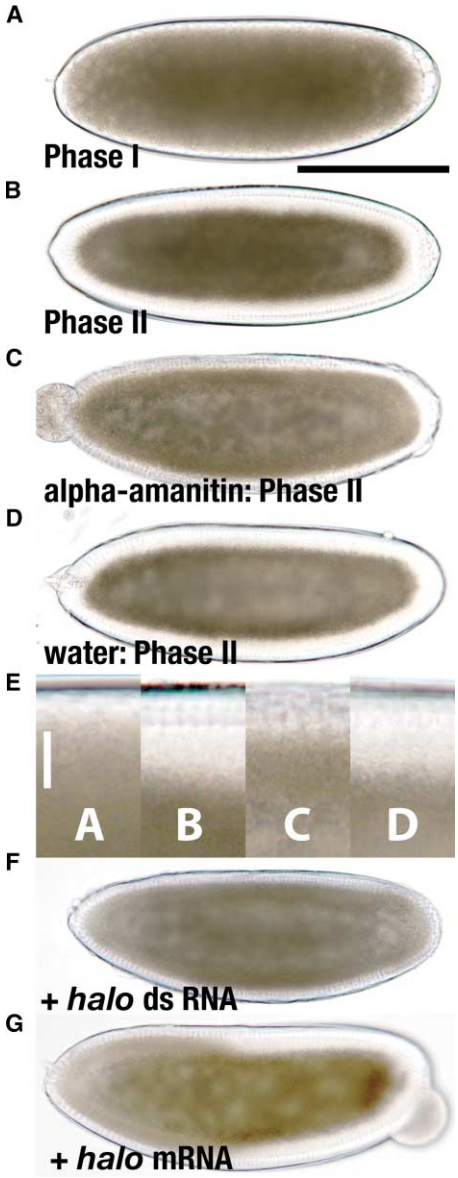

Figure 1. Cytoplasmic Clearing Is Abolished by α-Amanitin or RNA Interference; Clearing Is Restored in Δ(*halo*) Embryos by *halo* mRNA

(A–E) Alpha-amanitin prevents clearing. Wild-type embryos during phase I (A) or phase II (B, C, and D). Embryos were not injected (A and B), injected with α-amanitin (C) at 500 μl/ml in water, or injected with water alone (D). In the presence of α-amanitin, the periphery of the embryo fails to become transparent in phase II. The scale bar in (A) represents 200 μm. (E) Higher-magnification view of the periphery of the embryos from (A)–(D); the scale bar represents 20 μm. (F) Embryo injected with *halo* dsRNA during cleavage stages and analyzed during phase II; a *halo*-like clearing defect develops. (G) A Δ(*halo*) embryo injected with in vitro-synthesized *halo* mRNA; clearing is restored in the posterior half of the embryo, near the injection site (right).

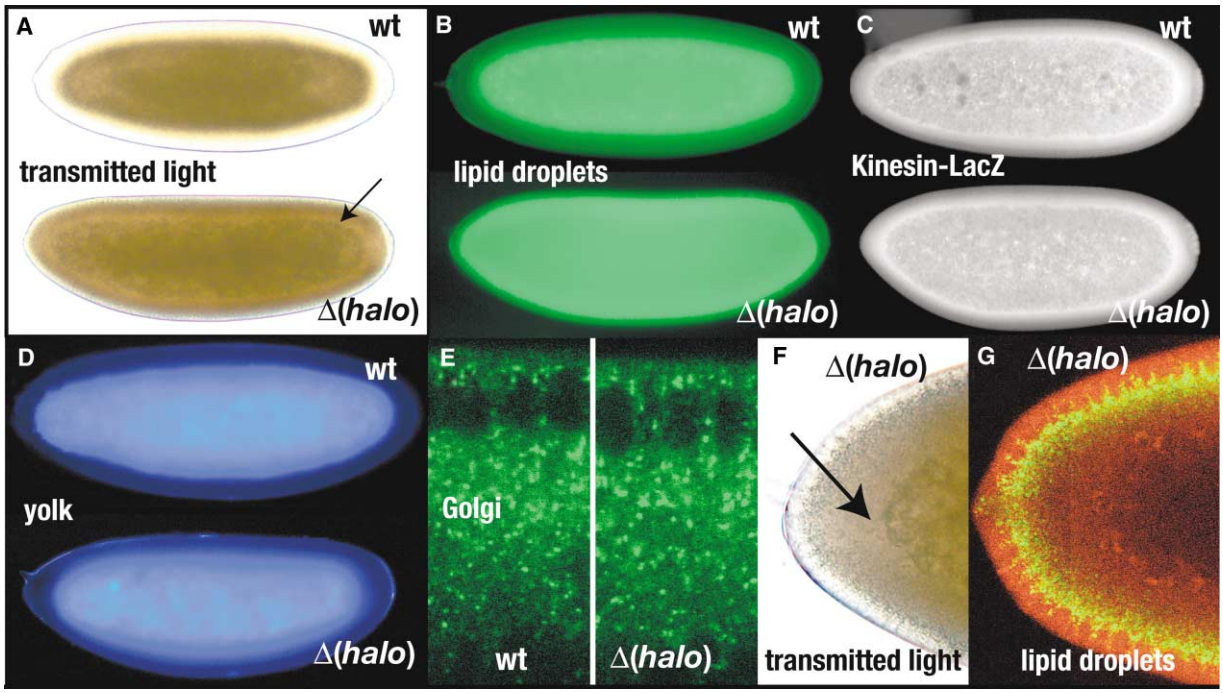

Figure 2. In Phase II, Halo Specifically Alters the Distribution of Lipid Droplets

All images show embryos in early to mid-cycle 14. Panels (A)–(D) compare the wild-type (top) and Δ(*halo)* (bottom) at the whole-embryo level. Panels (E), (F), and (G) show detailed views at higher magnification. (A and F) Overall embryo transparency in transmitted light. The arrows point to the "second halo," a cleared zone around the central yolk. (B and G) Lipid droplets were stained with the droplet-specific fluorescent dye Nile Red and inspected by epifluorescence (B) or confocal (G) microscopy. In (G), yellow represents lipid droplets, and red is a diffuse cytoplasmic signal that makes it possible to determine the outline of the embryo. (C) To mark microtubule plus ends, we used females expressing a kinesin-LacZ fusion protein in their germ line. Their embryos were stained for LacZ. (D) Yolk vesicles, detected via their autofluorescence by epifluorescence microscopy. (E) Distribution of the Golgi-associated protein Lava Lamp in the peripheral region (from the apical surface to the outer boundaries of the central yolk) of wild-type (left) and Δ(*halo)* (right) embryos, recorded by confocal microscopy. (F and G) In Δ(*halo)* embryos, lipid droplets accumulate apically, just under the nuclei, as shown by bright-field microscopy (F) and Nile Red staining for lipid droplets (G).

halo [9]. Basal depletion leads to a cleared region (a "second halo") around the central yolk (arrow in Figures 2A and 2F). Thus, in the absence of *halo*, not only is clearing not initiated in phase II, but net transport is also reversed.

This mislocalization of lipid droplets is progressive. At the beginning of phase I, embryos of the two genotypes appear to be similar, but they develop striking differences during phase II. Using a new method to display embryo opacity (Figure S2 in the Supplemental Data available with this article online), we find that as early as cycle 12, embryos that lack *halo* differ from wild-type embryos. This is due to early zygotic expression (Figure S2C).

Halo Alters the Physical Parameters of Droplet Motion

To understand how aberrant droplet distributions arise when *halo* is missing, we examined motion at the individual-droplet level. Droplets frequently switch travel direction in both wild-type and Δ(*halo)* embryos. We therefore tracked droplets in both genotypes and quantified the physical parameters of motion (Table 1).

In cycle 12 (phase I), plus-end motion in both genotypes was the same: mean travel distances and velocities were statistically indistinguishable. In the wild-type, plus-end transport increased significantly from phase I to phase II. This failed to occur in the absence of Halo. Travel velocities were not obviously altered. Thus, Halo is necessary for setting the correct travel distances for plus-end travel, specifically in phase II, and possibly controls the mechanism that turns off plus-end motors and simultaneously turns on minus-end motors [6]. For minus-end travel, travel distances were increased in Δ(*halo*) in both phase I and II to a similar extent, whereas velocities were again normal. Thus, reversed net transport in phase II Δ(*halo*) embryos results from a combination of increased minus- and decreased plus-end travel distances.

In the wild-type, two travel states can be distinguished for both directions of travel: a short-slow state (low velocities, short travel distances) and a long-fast state (higher velocities, longer travel distances) [6]. Δ(*halo*) embryos displayed these travel states for both directions, based on the previously established criteria [6, 7]: run lengths were well described by the sum of two exponentials (Table 1, χ^2), and short runs had a mean velocity approximately half that of long runs (data not shown). In Δ(*halo)* phase II embryos, the average travel distance of long-fast runs was increased in the minus-end direction and decreased in the plus-end direction. Thus, Halo controls run lengths in the long-fast travel state.

Long-fast travel states can be further characterized

Table 1. Physical Parameters of Droplet Motion

	Mean Travel Distance, nm	D_s, nm	D_L, nm	χ^2, $P(\chi^2)$	Number Ratio R_{SL}	Velocity, nm/s
Plus End						
Wild-type phase I (n = 287)	500 ± 40	60 ± 10	800 ± 100	0.57, 0.75	1.7 ± 0.7	335 ± 9
Δ(*halo*) phase I (n = 159)	480 ± 50	48 ± 10	900 ± 100	4.29, 0.002	2 ± 1	340 ± 10
Wild-type phase II (n = 1230)	750 ± 30	84 ± 6	1210 ± 90	0.80, 0.81	1.4 ± 0.3	342 ± 5
Δ(*halo*) phase II (n = 618)	560 ± 30	73 ± 7	1000 ± 100	1.18, 0.25	1.7 ± 0.4	313 ± 7
Minus End						
Wild-type phase I (n = 284)	600 ± 60	80 ± 10	1100 ± 200	0.54, 0.74	2.1 ± 0.9	380 ± 10
Δ(*halo*) phase I (n = 190)	760 ± 80	70 ± 10	2100 ± 600	1.83, 0.09	3 ± 2	430 ± 20
Wild-type phase II (n = 1294)	730 ± 30	82 ± 5	1250 ± 90	1.01, 0.45	1.6 ± 0.3	419 ± 7
Δ(*halo*) phase II (n = 755)	920 ± 40	85 ± 7	1700 ± 200	1.20, 0.19	1.5 ± 0.3	410 ± 8

Droplet motion was characterized by tracking analysis. Centroid-based image processing was used to determine droplet location as a function of time, and then custom software was used to parse the motion into pauses and "runs," i.e., periods of uninterrupted motion in a given direction. The distance constants D_S and D_L measure the average travel distance in the short-slow and long-fast travel states, respectively [6]. They result from fitting histograms of travel distance, D, to the sum of two decaying exponential functions: $y(D) = A_s e^{-D/D_3} + A_L e^{-D/D_L}$. The goodness of this fit is indicated by the χ^2 values and their corresponding probabilities. The number ratio R_{SL} measures the relative frequency of the short-slow relative to the long-fast travel state [6].

with an optical trap to stall individual moving droplets in the embryo. We determine a stall force, i.e., the mean force required to stop a moving droplet [3, 6]. This gives information about how many motors are simultaneously powering droplet motion, as well as about interactions between motors [3, 7]. In the wild-type, stall forces change during development but the forces for plus- and minus-end motion are always balanced [3]. In phase I, forces in wild-type and Δ(*halo)* embryos were indistinguishable for both directions of motion (Figure 3A). In phase II, stall forces in Δ(*halo)* were altered for both directions, resulting in unbalanced forces (Figure 3B); more minus-end moving and fewer plus-end moving droplets escaped from the trap than in the wild-type.

Molecular Identification of *halo*

Using deletions, we molecularly mapped *halo* to within 63 kbp (Figure S1). Eight genes are predicted in this chromosomal region. To determine which of these candidates was *halo*, we abolished their function individually by using double-stranded RNA interference [10]. Only for embryos injected with dsRNA against *CG7428* did we observe a disruption of clearing. In phase II, many developed a striking *halo*-like clearing defect (Figure 1F) and even displayed the second halo of a cleared region around the yolk. Because *CG7428* dsRNA phenocopies the *halo* clearing defect, we conclude that *CG7428* is *halo*.

In early embryos, we detected a single band for the *halo* message on Northern blots (approximately 800 nucleotides, not shown). These transcripts include the entire predicted coding region because we detected amplification products of the correct size by RT-PCR by using primers 5′ to the predicted start codon and 3′ to the predicted stop codon, respectively (Figure 4A and data not shown). The predicted protein (150 amino acids) is highly basic (pI = 10.2) and has no hydrophobic stretches reminiscent of a signal sequence or transmembrane domain.

Halo Expression Is Highly Dynamic

To determine when *halo* was expressed, we performed in situ hybridization with *halo*-specific probes (Figure 5). Signal was almost absent in control experiments performed in parallel, i.e., in wild-type embryos hybridized with sense probes and in Δ(*halo)* tested with anti-sense probes (not shown). In the wild-type, *halo* message was undetectable in cleavage stages (i.e., indistinguishable from background) and had very low levels at the beginning of phase I. Levels in cycle 12 were slightly above background (not shown). Signal increased modestly for cycle 13 embryos, and levels were very high at the beginning of cycle 14, before nuclear elongation. During nuclear elongation and early membrane invagination, the signal faded in a dorsal-ventral gradient. It dropped precipitously just after the membranes reached the tip of the nuclei. Afterwards, *halo* signal persisted at low levels for many hours in a dynamic pattern (Figure S3A).

Evolutionary Conservation of Halo

By BLAST, we detected no sequences with significant similarity to Halo in non-Dipteran species or the mosquito *Anopheles gambiae*. However, the genome of *Drosophila pseudoobscura* might encode a protein very similar to Halo; it aligned almost perfectly (nine amino acid changes over a 109 amino acid stretch, Figure 4B) with the last two-thirds of the Halo ORF, starting with a second, in-frame start codon. By in situ hybridization, this candidate *halo* homolog was transiently expressed like *halo* just before cellularization (Figure S4A), and injection of dsRNA against this sequence prevented

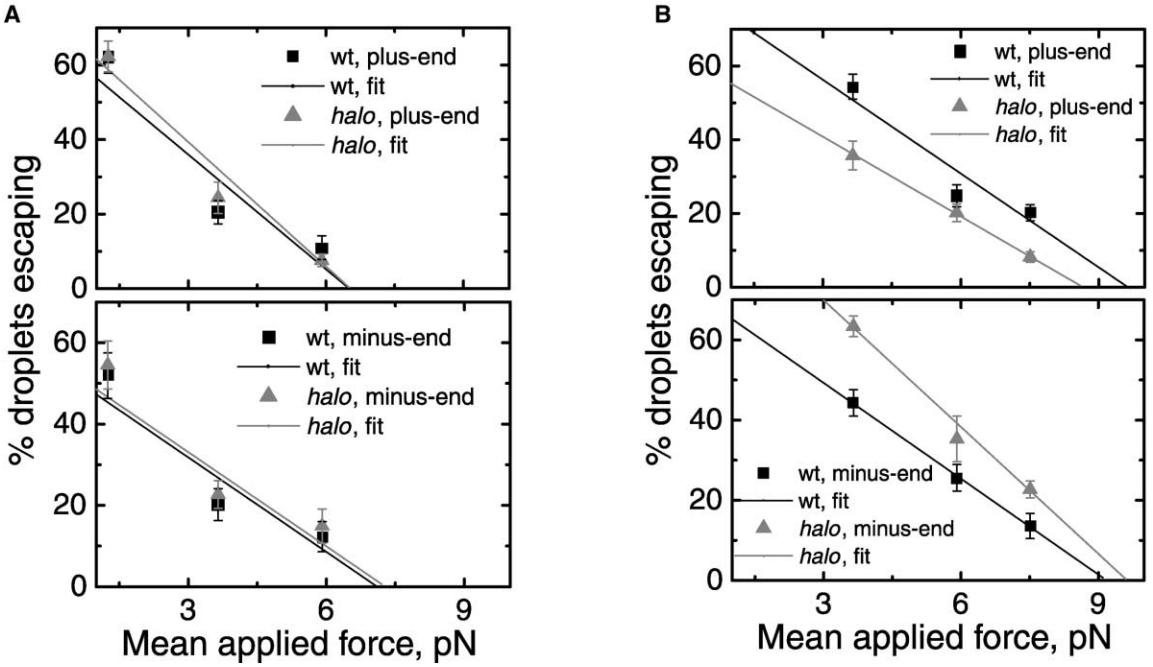

Figure 3. Droplet Stall Forces

The panels show the percentage of droplets stalled as a function of force applied by optical tweezers in wild-type versus Δ(*halo*). (A) Phase I. (B) Phase II. Top panels are for plus-end moving droplets, bottom panels for minus-end moving droplets.

clearing (Figure S4B). We conclude that we have identified the homolog of *halo* in *D. pseudoobscura*, *Dps/halo*, and that the function of Halo has been conserved for at least 46 million years [11].

The comparison with Dps/Halo suggested that only the C-terminal 109 amino acids of Dmel/Halo are required to determine transport directionality. We generated in vitro-capped and polyadenylated RNA encoding this shorter ORF and injected it into Δ(*halo*) embryos. In the vast majority of embryos, the mutant phenotype was partially rescued, and clearing occurred near the injection site (Figure 1G). When embryos were injected in phase II, noticeable clearing was observed within 10 min. In wild-type embryos injected toward the end of phase II, clouding failed to occur near the injection site during gastrulation (not shown), suggesting that ectopic expression of Halo interferes with the switch from net plus- to net minus-end transport.

Proteins Similar to Halo

Six additional predicted *D. melanogaster* proteins could be aligned to Halo and Dps/Halo in a common core domain (Figures 4C and 4D). At least five of these Halo-like genes have sequences with high similarity in *D. pseudoobscura*. Of the 73 core domain residues, 39 are identical in a majority of the 13 family members, and five residues are invariant.

To determine if these predicted genes were expressed, we performed in situ hybridizations with early *D. melanogaster* embryos. All family members were transiently upregulated during syncytial or cellular blastoderm stages (Figures S3B and S3C; data not shown). For example, *HL3* was expressed in broad rings during cycle 13 and early 14, and levels dropped to background by the end of cellularization. *HL6* showed a seven-stripe pattern during mid-cycle 14 and was specifically upregulated in ventral regions that give rise to the ventral furrow.

Discussion

In this paper we identify a novel protein, Halo, that functions as a transport directionality factor. In its absence, droplet transport is biased toward minus ends; in its presence, transport is biased toward plus ends. Control of transport directionality is as yet poorly understood but is of general relevance because many cargoes, including axonal vesicles, mitochondria, melanosomes, neurofilaments, RNP granules, and viruses, move bidirectionally along microtubules [2, 4, 5, 12–14].

Halo is zygotically expressed and acts on the pre-existing transport machinery to control net direction. Halo probably remains tightly bound to its targets or is rapidly degraded so that it cannot spread effectively through the embryo because we observe embryos with localized clearing defects when Halo function is locally abolished by RNA interference (not shown) or when Halo is locally provided by injected mRNA (Figure 1G).

Functionally, Halo both upregulates plus-end motion and downregulates minus-end motion, and the stall force measurements suggest that this is in part due to increasing the average number of engaged plus-end motors and decreasing the number of engaged minus-end motors (see Supplemental Data). Based on these observations, we have developed a speculative model for Halo's function (Figure 6).

Name	Short name	size (aa)	aa identity to Halo in core	aa identity with *Dps* homolog	pI *Dmel* / *Dps*
Halo	Halo	150	100%	92% * / 96%	10.1 / 10.3
CG13716	HL1	117	40%	54% / 74%	10.2 / 11.0
CG13713	HL2	99	37%	73% / 92%	10.2 / 10.8
CG15876	HL3	138	32%	67% / 89%	10.5 / 11.0
CG13712	HL4	117	27%	60% / 74%	10.1 / 11.3
CG13711	HL5	127	32%	N.D.	10.1 / N.D.
CG14112	HL6	146	33%	65% / 74%	10.5 / 10.4

Figure 4. Mapping and Evolutionary Conservation of Halo

(A) Schematic representation of *halo* region. The predicted ORF for Halo is indicated. Primers used for synthesizing RNAs for in situ hybridization and RNAi are in red. The most-5′ and -3′ primers used to detect *halo* message by RT-PCR are in green. Blue indicates the extent of the putative *halo* transcribed region, based on cDNAs sequenced by the Berkeley *Drosophila* Genome Project (BDGP) (full line) and our RT-PCR results (broken line). The exact 5′ end of the message has not been determined.

(B) Alignment of the predicted protein sequences for Halo from *D. melanogaster* (mel) and *D. pseudoobscura* (ps). Residues common in both sequences are underlayed in orange. The methionine indicated by a star may represent an alternative start codon in the *D. melanogaster* message.

(C) Alignment of Halo family members. The predicted Halo-like proteins from *D. melanogaster* (mel) and *D. pseudoobscura* (ps) were aligned and showed extensive similarity in a 73 amino acid "core domain" (shown). The consensus displays an amino acid for a particular position if seven or more of the 13 proteins share this residue. Color code: orange indicates that the residue is identical for all family members; blue indicates that the residue is not invariant but the same as the consensus; and purple indicates that the residue falls into the same chemical group as the amino acid in the consensus (aliphatic, aromatic, basic, etc).

(D) Properties of Halo-like proteins. Size is the predicted number of amino acids. Percentage identity, over the full length and within the core domain (see C), was determined for various combinations (an asterisk indicates that analysis was over the C-terminal 109 amino acids; see [B]). pI = isoelectric point. N.D. = no data.

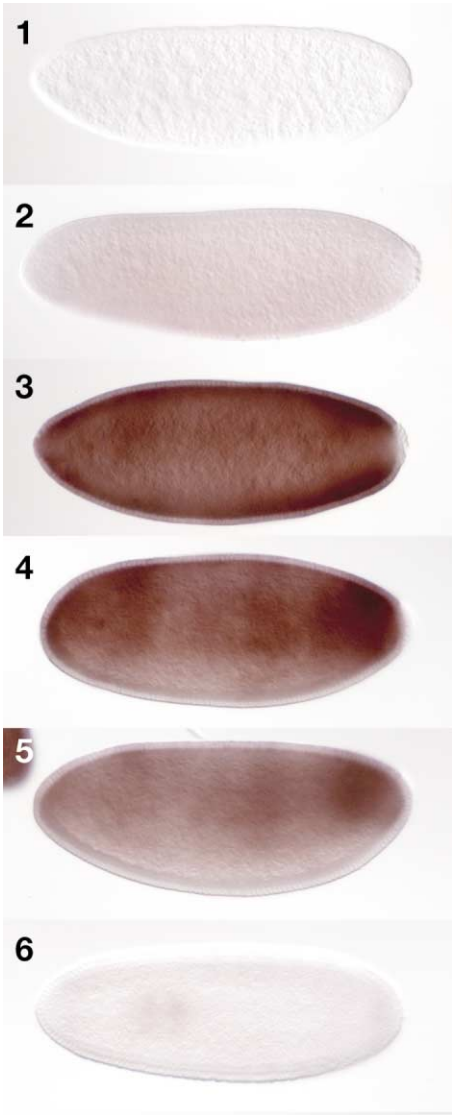

Figure 5. Time Course of *D. melanogaster halo* Expression Detected by In Situ Hybridization

(1) Early phase I; (2) cycle 13; (3) cycle 14, no nuclear elongation; (4) cycle 14, membrane invagination has started; (5) cycle 14, membranes have reached the base of nuclei; (6) cycle 14, membranes are about 50% beyond the base of nuclei.

Model of Halo function

We hypothesize that Halo regulates the conformation of the previously proposed switching complex [6], the machinery that coordinates opposite-polarity motors and terminates runs. Both functions may rely on how efficiently this machinery presents motors to the microtubule tracks [15]. We propose that Halo induces a conformation that causes less-efficient presentation of minus-end motors and more-efficient presentation of plus-end motors. For example, this conformation might pull minus-end motors slightly off the microtubule track and push plus-end motors toward the track (Figure 6).

For minus-end travel, when the minus-end motors are engaged, this pushing and pulling would have two effects: (1) runs would terminate more frequently because the probability of motors coming off the track would be increased, and (2) stall forces would decrease because on average fewer motors are simultaneously bound to the track. This explains why in the presence of Halo minus-end runs are shorter and stall forces lower. Conversely, during plus-end travel, Halo would cause longer runs and higher stall forces because the plus-end motors are pushed closer toward the tracks.

A Transacting Factor for Developmental Transitions

At the transition from phase I to phase II, droplet transport undergoes profound changes; forces are upregulated and plus-end travel lengths increase. Halo is likely to be important for the developmental signals that bring about this transition because it is highly upregulated at that time, because in its absence this transition does not occur correctly, and because exogenously provided Halo promotes net inward transport (Figure 1G).

Because even in the absence of Halo there is a distinct transition in droplet motion from phase I to phase II, there must be a second signal (signal X) that promotes net outward transport. In wild-type phase II, net inward transport dominates and results in clearing. In the absence of Halo, signal X leads to net outward transport. To allow net outward, minus-end transport in phase III in the wild-type, it may be necessary to remove the Halo-dependent signal—consistent with the rapid downregulation of *halo* message in the middle of phase II. Indeed, forced expression of Halo at the end of phase II prevents the switch to net outward transport.

Unlike the Halo-dependent signal, signal X does not require zygotic transcription because α-amanitin-injected embryos display net minus-end transport in phase II. Signal X might be mediated by a kinase cascade similar to the one described for regulation of pigment-granule motion. Conversely, as a result of kinase activity, a protein similar to Halo (in function, if not in primary sequence) could be recruited to pigment granules and thus alter the balance of motor activity and reverse transport direction.

A Family of Related Regulators

The Halo family in *Drosophila* consists of small, basic proteins that are zygotically expressed in distinct domains during blastoderm stages. As their expression changes dynamically over short periods, family members are probably needed at very specific times.

The Halo-like proteins probably control the transport of cargoes other than droplets because embryos that lack the left arm of chromosome III (where HL1 through H6 are located) have no obvious defects in cytoplasmic clearing ([9]; our unpublished observations). Because the whole family has been maintained by evolution, different family members probably have distinct functions. Each member may set net directionality for a different organelle, thus allowing the cell to independently control the transport of distinct cargoes.

Currently, Halo-like factors are only known in *Drosophila*. Although this family might represent a novel type of regulator only found in fruit flies, it is also possible that functionally similar regulators are widespread but that their primary sequence evolves so rapidly that re-

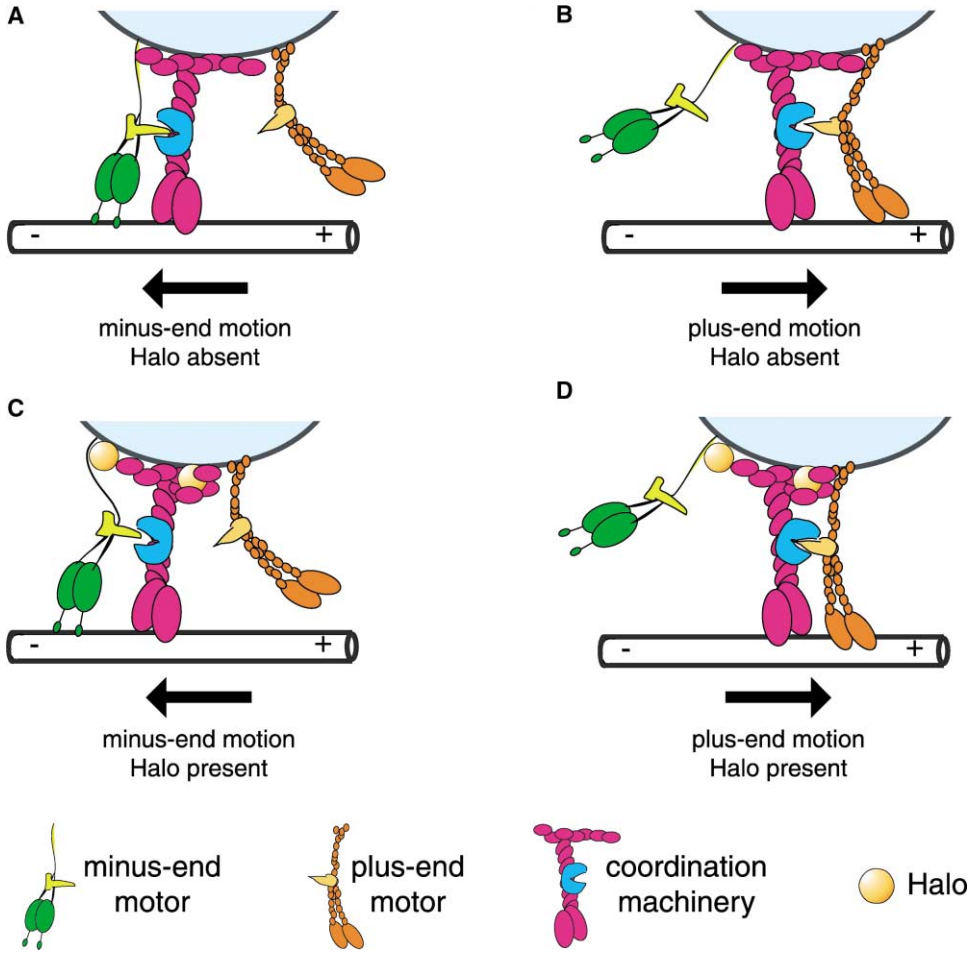

Figure 6. Model for Halo Action

Top panels (A and B) show motion without Halo; bottom panels (C and D) show motion in the presence of Halo (yellow ball). The model (based on [18]) assumes that the activity of opposite-polarity motors is coordinated so that plus-end motors (orange) are not engaged with the tracks during minus-end motion (A and C) and that minus-end motors (green) are not engaged during plus-end motion (B and D). Coordination is achieved by motors binding alternately to the coordination machinery (purple). The dynein cofactor dynactin may be part of this machinery [6, 18, 19] . Halo sterically interferes with the minus-end motor (C), weakening its binding to the coordination machinery. Halo promotes tighter binding of the plus-end motor to the coordination machinery and thus more effective presentation of the motors to the tracks (D), possibly by altering the conformation of the coordination machinery.

lated molecules in distant species are not straightforward to recognize.

Conclusions

Our analysis of Halo shows how a cell can control the net direction of bidirectionally moving cargoes by controlling expression of a single protein. Because Halo influences the run lengths of both plus- and minus-end motors, Halo probably acts on the machinery that mediates motor coordination. This machinery remains ill defined but is crucial for understanding how net transport is regulated [1]. Analysis of Halo should provide an inroad for molecularly dissecting this machinery, for example by determining the proteins with which Halo physically interacts. In addition, because Halo is required for balancing forces produced by opposite-polarity motors on the same cargo (Figure 3B), analyzing Halo should help uncover the as-of-yet entirely unknown mechanisms that regulate force production in vivo.

For development, the Halo family may provide crucial insight into how cellular polarity is established and maintained. Despite great progress toward understanding the initial polarity cues (reviewed in [16]), how the cell translates a polarized cytoskeleton into actual cellular reorganization remains poorly understood. Control of transport by Halo-like proteins and similar factors provides such a link.

Experimental Procedures

Fly Stocks

Oregon-R was the wild-type stock. Unless otherwise noted, fly stocks, mutant chromosomes, and break-point data for deletions are as described on FlyBase (http://flybase.bio.indiana.edu). To construct the synthetic deficiency $\Delta(halo)$, we combined the deletion $Df(2L)dp^{79b}$ (break points 22A2-3; 22D5-E1) and the duplication $Dp(2;2)dpp^{d21}$ (break points 22A2-3; 22F1-2; inserted at 52F) onto a single chromosome. *D. pseudoobscura* stock 14011-0121.34 was from the Tucson *Drosophila* Species Stock Center.

Embryo Injections

Embryos were injected according to standard procedures [17]. To inhibit zygotic transcription, we injected α-amanitin dissolved in water at 500 μg/ml. For RNA interference experiments, we generated dsRNA in vitro (approximately 1 μg/μl) by using established procedures [10] and injected embryos before cellularization.

To rescue the Δ*(halo)* mutant phenotype, we generated a chimeric template for in vitro transcription. It includes a SP6 promotor, 5′ UTR of *Xenopus* β-globin, Halo ORF (from the second AUG to the stop codon), 3′ UTR of *Xenopus* β-globin, and a PolyA stretch. Capped mRNA was produced with the mMESSAGE mMACHINE-SP6 kit (Ambion) and injected at concentrations of approximately 7 μg/μl.

Particle Tracking and Analysis

Droplet motion was recorded and quantitated essentially as described [3, 6]. See Supplemental Data for details.

Acknowledgments

We thank E. Wieschaus, W. Gelbart, R. Ray, the Bloomington Stock Center, and the Tucson *Drosophila* Species Stock Center for fly stocks. M.A.W. thanks S.L. Lovett for advice on sequence analysis and M. Barlow, C. Bell, and H. Balcer for expert technical assistance. We thank J. Sisson for antibodies, T. Tange for help with creating mRNA in vitro, and M. Postner and E. Wieschaus for their data on the initial deletion mapping of *halo*. We are grateful to J. Gelles, K. White, P. Sengupta, E. Rubinstein, and E. Wieschaus for comments on the manuscript. This work was supported by NIGMS grants GM64687-01A1 to MAW and GM-64621-01 to S.P.G., and M.A.W. gratefully acknowledges that work in his laboratory is supported by a Kimmel Scholar Award from the Sidney Kimmel Foundation for Cancer Research. Confocal microscopy was made possible by the National Institutes of Health SIG grant S10RR16780.

Received: July 14, 2003
Revised: August 14, 2003
Accepted: August 14, 2003
Published: September 30, 2003

References

1. Vale, R.D. (2003). The molecular motor toolbox for intracellular transport. Cell *112*, 467–480.
2. Hollenbeck, P.J. (1996). The pattern and mechanism of mitochondrial transport in axons. Front. Biosci. *1*, d91–d102.
3. Welte, M.A., Gross, S.P., Postner, M., Block, S.M., and Wieschaus, E.F. (1998). Developmental regulation of vesicle transport in Drosophila embryos: forces and kinetics. Cell *92*, 547–557.
4. Suomalainen, M., Nakano, M.Y., Keller, S., Boucke, K., Stidwill, R.P., and Greber, U.F. (1999). Microtubule-dependent plus- and minus end-directed motilities are competing processes for nuclear targeting of adenovirus. J. Cell Biol. *144*, 657–672.
5. Tuma, M.C., and Gelfand, V.I. (1999). Molecular mechanisms of pigment transport in melanophores. Pigment Cell Res. *12*, 283–294.
6. Gross, S., Welte, M., Block, S., and Wieschaus, E. (2000). Dynein-mediated cargo transport in vivo: a switch controls travel distance. J. Cell Biol. *148*, 945–956.
7. Gross, S.P., Welte, M.A., Block, S.M., and Wieschaus, E.F. (2002). Coordination of opposite-polarity microtubule motors. J. Cell Biol. *156*, 715–724.
8. Edgar, B.A., Kiehle, C.P., and Schubiger, G. (1986). Cell cycle control by the nucleo-cytoplasmic ratio in early Drosophila development. Cell *44*, 365–372.
9. Merrill, P.T., Sweeton, D., and Wieschaus, E. (1988). Requirements for autosomal gene activity during precellular stages of Drosophila melanogaster. Development *104*, 495–509.
10. Kennerdell, J.R., and Carthew, R.W. (1998). Use of dsRNA-mediated genetic interference to demonstrate that frizzled and frizzled 2 act in the wingless pathway. Cell *95*, 1017–1026.
11. Powell, J.R. (1997). Progress and Prospects in Evolutionary Biology: The Drosophila Model (Oxford: Oxford University Press).
12. Carson, J.H., Cui, H., and Barbarese, E. (2001). The balance of power in RNA trafficking. Curr. Opin. Neurobiol. *11*, 558–563.
13. Shah, J.V., Flanagan, L.A., Janmey, P.A., and Leterrier, J.F. (2000). Bidirectional translocation of neurofilaments along microtubules mediated in part by Dynein/Dynactin. Mol. Biol. Cell *11*, 3495–3508.
14. Gilbert, S.P., and Sloboda, R.D. (1984). Bidirectional transport of fluorescently labeled vesicles introduced into extruded axoplasm of squid Loligo pealei. J. Cell Biol. *99*, 445–452.
15. Gross, S.P., Tuma, M.C., Deacon, S.W., Serpinskaya, A.S., Reilein, A.R., and Gelfand, V.I. (2002). Interactions and regulation of molecular motors in Xenopus melanophores. J. Cell Biol. *156*, 855–865.
16. Doe, C.Q., and Bowerman, B. (2001). Asymmetric cell division: fly neuroblast meets worm zygote. Curr. Opin. Cell Biol. *13*, 68–75.
17. Spradling, A.C. (1986). P-element mediated transformation. In Drosophila: A practical approach, First Edition, D.B. Roberts, ed. (Oxford: IRL Press), pp. 175–197.
18. Gross, S.P. (2003). Dynactin: coordinating motors with opposite inclinations. Curr. Biol. *13*, R320–R322.
19. Deacon, S.W., Serpinskaya, A.S., Vaughan, P.S., Fanarraga, M.L., Vernos, I., Vaughan, K.T., and Gelfand, V.I. (2003). Dynactin is required for bidirectional organelle transport. J. Cell Biol. *160*, 297–301.